Physica D 238 (2009) 2142–2152

Contents lists available at ScienceDirect

Physica D

journal homepage: www.elsevier.com/locate/physd

Sensitisation waves in a bidomain fire-diffuse-fire model of intracellular Ca^{2+} dynamics

R. Thul [a,*], S. Coombes [a], G.D. Smith [b]

[a] School of Mathematical Sciences, University of Nottingham, Nottingham, NG7 2GL, UK
[b] Department of Applied Mathematics, The College of William and Mary, Williamsburg, VA 23187, USA

ARTICLE INFO

Article history:
Received 14 May 2009
Received in revised form
11 August 2009
Accepted 17 August 2009
Available online 22 August 2009
Communicated by B. Sandstede

PACS:
87.10.-e
87.10.Ed
87.17.-d

Keywords:
Calcium wave
Fire-diffuse-fire
Standing front
Sensitisation
Evans function

ABSTRACT

We present a bidomain threshold model of intracellular calcium (Ca^{2+}) dynamics in which, as suggested by recent experiments, the cytosolic threshold for Ca^{2+} liberation is modulated by the Ca^{2+} concentration in the releasing compartment. We explicitly construct stationary fronts and determine their stability using an Evans function approach. Our results show that a biologically motivated choice of a dynamic threshold, as opposed to a constant threshold, can pin stationary fronts that would otherwise be unstable. This illustrates a novel mechanism to stabilise pinned interfaces in continuous excitable systems. Our framework also allows us to compute travelling pulse solutions in closed form and systematically probe the wave speed as a function of physiologically important parameters. We find that the existence of travelling wave solutions depends on the time scale of the threshold dynamics, and that facilitating release by lowering the cytosolic threshold increases the wave speed. The construction of the Evans function for a travelling pulse shows that of the co-existing fast and slow solutions the slow one is always unstable.
© 2009 Elsevier B.V. All rights reserved.

1. Introduction

The toolbox of intracellular Calcium (Ca^{2+}) plays a vital role in a multitude of cellular events. Ca^{2+} signals encode the beginning of fertilisation, control muscle contraction, respond to the loss of gravitational acceleration or co-ordinate programmed cell death [1,2]. This versatility derives from complex spatio-temporal patterns. Cells can restrict transient rises of the cytosolic Ca^{2+} concentration to a few micrometers or support whole cell responses that extend up to 1 mm. At the same time, Ca^{2+} signals last from tens of microseconds to 24 h. Cells achieve such high specificity by engaging several internal compartments like the nucleus or the endoplasmic/sarcoplasmic reticulum (ER/SR) in generating Ca^{2+} signals [3]. Although it is well known that these organelles store Ca^{2+} at high concentrations, their internal dynamics as well as their contributions to global cellular responses are just beginning to be unravelled [4–9]. In particular, a recent study in ventricular myocytes suggests a strong impact of Ca^{2+} in the SR on whole cell Ca^{2+} waves. Keller et al. [10] report that a localised decrease in luminal Ca^{2+}, i.e. Ca^{2+} in the ER or SR, leads to slower Ca^{2+} waves. Importantly, these spatially restricted changes in luminal Ca^{2+}occur on a fast time scale, which leaves the bulk SR Ca^{2+} concentration unchanged. Scalar models that focus on Ca^{2+}-induced-Ca^{2+} release (CICR) and that neglect the ER/SR are not consistent with this experimental observation, because these approaches predict an increase in wave speed for the same experimental protocol.

The local Ca^{2+} dynamics is governed by Ca^{2+} release from the ER/SR into the cytosol and re-sequestration. Ca^{2+} liberation occurs through two classes of ion channel: the inositol-1,4,5-trisphosphate (IP_3) receptor channel or the ryanodine receptor (RyR) channel. Both channel types share the property that the cytosolic Ca^{2+} concentration influences their conducting state. At basal Ca^{2+} con centrations, channels rarely open. However, a small increase in cytosolic Ca^{2+} leads to a significant increase of the open probability [11]. This autocatalytic step is the mechanistic basis of CICR. In the opposite direction, sarco(endo)plasmic reticulum Ca^{2+} ATPase (SERCA) pumps transport Ca^{2+} back from the cytosol to the lumen of the ER/SR. Blocking SERCA pumps acutely then raises the cytosolic Ca^{2+} concentration, so that without any ER/SR dynamics CICR leads to larger open probabilities, which in turn leads to waves of Ca^{2+} with higher velocities.

* Corresponding author. Tel.: +0044 115 84 67913; fax: +0044 115 95 13837.
E-mail addresses: ruediger.thul@nottingham.ac.uk (R. Thul), stephen.coombes@nottingham.ac.uk (S. Coombes), greg@as.wm.edu (G.D. Smith).

0167-2789/$ – see front matter © 2009 Elsevier B.V. All rights reserved.
doi:10.1016/j.physd.2009.08.011

For inefficient SERCA pumps, Ca^{2+} accumulates in the cytosol and its concentration in the lumen decreases. Taking into account that RyR channels express Ca^{2+} binding sites in the SR [12], the results in [10] suggest a feedback of the luminal Ca^{2+} concentration on the open probability of the RyR channel. A decrease in SR Ca^{2+} desensitises ion channels and hence can reduce wave speed. Note that such a desensitisation results from a spatially confined decrease in SR Ca^{2+} and not from a lower bulk Ca^{2+} concentration in the SR [13]. In the present mathematical study, we show how luminal Ca^{2+} shapes travelling waves. This provides strong evidence for slower Ca^{2+} waves when the local Ca^{2+} concentration in the SR is low. Moreover, our analysis reveals a novel nonlinear mechanism to stabilise stationary fronts that would otherwise be unstable.

Although the findings in [10] motivate our analysis, our results are not restricted to ventricular myocytes. First, Ca^{2+} waves have been observed in various cell types such as *Xenopus* oocytes [14–16], atrial mycoytes [17], smooth muscle cells [18] or HeLa cells [19]. Morevoer, CICR is the dominant cytosolic process underlying all these waves, and IP_3R channels are known to express luminal binding sites for Ca^{2+} as well [20]. To account for this universality, our model consists of two parts: a framework to represent CICR and a luminal feedback mechanism to modulate the open probability of Ca^{2+} releasing channels.

We implement CICR through a threshold process. It captures the notion of Ca^{2+} excitability in that Ca^{2+} liberation only starts reliably if the cytosolic Ca^{2+} concentration exceeds a given threshold. Threshold models have been successfully applied to study transitions from saltatory to continuous wave propagation [21–23] or stochastic release dynamics in one and two dimensions [24–26]. These single domain threshold models treat the ER/SR as an infinite store so that release events do not change the luminal Ca^{2+} concentration. Following recent work [27,28], we here employ a bidomain threshold model that incorporates dynamics in both the cytosol and the lumen:

$$\frac{\partial c}{\partial t} = D\frac{\partial^2 c}{\partial x^2} + J_{\mathrm{rel}}(c, c_{\mathrm{er}}) - J_{\mathrm{pump}}(c, c_{\mathrm{er}}), \tag{1a}$$

$$\frac{\partial c_{\mathrm{er}}}{\partial t} = D_{\mathrm{er}}\frac{\partial^2 c_{\mathrm{er}}}{\partial x^2} - \gamma^{-1}[J_{\mathrm{rel}}(c, c_{\mathrm{er}}) - J_{\mathrm{pump}}(c, c_{\mathrm{er}})], \tag{1b}$$

where c and c_{er} denote the cytosolic and luminal Ca^{2+} concentration, respectively, for $(x, t) \in \mathbb{R} \times \mathbb{R}^+$, and the parameter γ refers to the volume ratio between the ER and the cytosol. For notational convenience, we drop the distinction between the ER and SR and refer to these intracellular Ca^{2+} stores as the ER from now on. Ca^{2+} diffuses in both the cytosol and the lumen with effective diffusion coefficients D and D_{er}, respectively. The release current J_{rel} is given by

$$J_{\mathrm{rel}}(c, c_{\mathrm{er}}) = (c_{\mathrm{er}}(x, t) - c(x, t)) \sum_m \eta(t - T^m(x)). \tag{2}$$

Here, $\eta(t)$ describes the release shape and depends on the release times $T^m(x)$, where the superscript counts successive release events at a point x. Release times are defined via

$$T^m(x) = \inf\{t \mid c(x, t) \geq c_{\mathrm{th}}(x, t), t > T^{m-1}(x) + \tau_R\}, \quad m = 0, 1, \ldots. \tag{3}$$

Ca^{2+} liberation can only occur if the concentration in the cytosol reaches the cytosolic threshold $c_{\mathrm{th}}(x, t)$ and if the time difference between successive release initiations is larger than the refractory period τ_{R}. The current J_{pump} reflects the impact of SERCA pumps, which we model as [28]

$$J_{\mathrm{pump}}(c, c_{\mathrm{er}}) = \frac{c}{\tau} - \frac{c_{\mathrm{er}}}{\tau_{\mathrm{er}}}. \tag{4}$$

To incorporate the luminal feedback onto the open probability, we make the threshold in the cytosol space and time dependent:

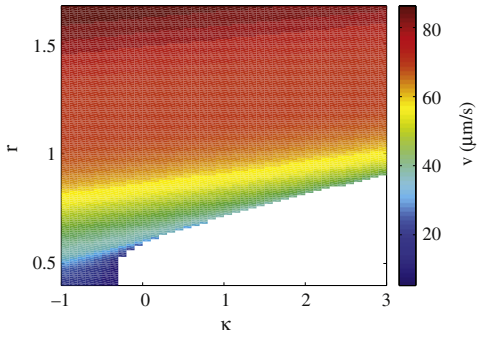

Fig. 1. Wave speed v of a travelling pulse as a function of the strength of threshold accommodation κ when we re-scale both pump time scales, τ and τ_{er}, by a common factor r. The values at $r = 1$ are listed below. See text for details. Parameter values are $D = 30\ \mu\mathrm{m}^2\ \mathrm{s}^{-1}$, $\Delta = 0.05$ s, $\tau = 0.01$ s, $D_{\mathrm{er}} = 5\ \mu\mathrm{m}^2\ \mathrm{s}^{-1}$, $\tau_{\mathrm{er}} = 10$ s, $\overline{\eta} = 1\ \mathrm{s}^{-1}$, $c_{\mathrm{th}}^0 = 0.4\ \mu$M, $c_{\mathrm{th}}^{\mathrm{er}} = 119.5\ \mu$M, $c_T^\infty = 20\ \mu$M, $\tau_{\mathrm{th}} = 1$ s, and $\gamma = 0.167$. The release duration Δ is defined after Eq. (25).

$$\frac{\partial c_{\mathrm{th}}}{\partial t} = D_{\mathrm{th}}\frac{\partial^2 c_{\mathrm{th}}}{\partial x^2} - \frac{1}{\tau_{\mathrm{th}}}\left(c_{\mathrm{th}} - c_{\mathrm{th}}^0\right) + \frac{\kappa}{\tau_{\mathrm{th}}}\Theta\left(c_{\mathrm{er}} - c_{\mathrm{th}}^{\mathrm{er}}\right). \tag{5}$$

We include a diffusive contribution to the threshold dynamics to study a wider class of luminal feedback mechanisms. For instance, luminal buffers such as calsequestrin are known to modulate the open probability of RyR channels [29–32]. $D_{\mathrm{th}} > 0$ corresponds to an effective diffusion coefficient that could arise through the diffusion of luminal Ca^{2+} buffers. Note that D_{th} only refers to the threshold dynamics and is not to be confused with the effective diffusion coefficients that govern the time evolution of the cytosolic and luminal Ca^{2+} concentration in the presence of buffers. See [33–40] for further details on buffers dynamics. In Section 3, we will set $D_{\mathrm{th}} = 0$ to focus on local regulation in the lumen only. In the absence of any feedback the local dynamics relaxes to some background value c_{th}^0 on a time scale τ_{th}. The impact of the luminal Ca^{2+} concentration is encoded by the last term, where Θ denotes the Heaviside function that is 1 for non-negative arguments and 0 otherwise. As soon as the Ca^{2+} concentration in the ER exceeds some threshold $c_{\mathrm{th}}^{\mathrm{er}}$, the cytosolic threshold either increases or decreases depending on the sign of κ. The modulus of κ controls the strength of the feedback, where a larger value corresponds to a stronger accommodation. The notion of luminal control of a cytosolic threshold (Eq. (5)) is consistent with experimental findings of calsequestrin interacting with Ca^{2+} releasing channels [32,41]. Note that a negative value of κ presents an increased tendency to liberate Ca^{2+} when ER Ca^{2+} increases above the luminal threshold $c_{\mathrm{th}}^{\mathrm{er}}$ and hence corresponds to a sensitisation of intracellular Ca^{2+} channels, whereas a positive value of κ reflects desensitisation.

Fig. 1 illustrates how varying the strength of Ca^{2+} sequestration alters the wave speed of a travelling pulse for various values of κ. We re-scaled both time scales, τ and τ_{er}, by the same factor r, so that the total Ca^{2+} concentration c_T^∞ in the wake and in the front of the pulse remains unchanged [28]. Thus, an acute decrease in SERCA activity as performed experimentally in [10] corresponds to decreasing r in Fig. 1. Consistent with these experimental findings, energising pumps ($r < 1$) leads to slower waves; however, this occurs for positive as well as negative values of κ and thus is not specific to sensitisation. The white region in Fig. 1 represents propagation failure, which is consistent with earlier results that waves do not exist for very strong pumps [42]. On the other hand, less efficient pumps ($r > 1$) give rise to faster waves. Since the wave speed behaves similarly for a broad range of pump strengths, we use the value of τ and τ_{er} at $r = 1$ throughout the manuscript.

As seen in Fig. 1 and elsewhere in this study, small changes in κ can have significant consequences for wave dynamics. In

Download English Version:

https://daneshyari.com/en/article/10735984

Download Persian Version:

https://daneshyari.com/article/10735984

Daneshyari.com